

Modeling the Newtonian Dynamics for Rotation Curve Analysis of Thin-Disk Galaxies

James Q. Feng and C. F. Gallo

Superconix Inc, 2440 Lisbon Avenue, Lake Elmo, MN 55042, USA; info@superconix.com

Received [year] [month] [day]; accepted [year] [month] [day]

Abstract We present an efficient, robust computational method for modeling the Newtonian dynamics for rotation curve analysis of thin-disk galaxies. With appropriate mathematical treatments, the apparent numerical difficulties associated with singularities in computing elliptic integrals are completely removed. Using a boundary element discretization procedure, the governing equations are transformed into a linear algebra matrix equation that can be solved by straightforward Gauss elimination in one step without further iterations. The numerical code implemented according to our algorithm can accurately determine the surface mass density distribution in a disk galaxy from a measured rotation curve (or vice versa). For a disk galaxy with a typical flat rotation curve, our modeling results show that the surface mass density monotonically decreases from the galactic center toward periphery, according to Newtonian dynamics. In a large portion of the galaxy, the surface mass density follows an approximately exponential law of decay with respect to the galactic radial coordinate. Yet the radial scale length for the surface mass density seems to be generally larger than that of the measured brightness distribution, suggesting an increasing mass-to-light ratio with the radial distance in a disk galaxy. In a nondimensionalized form, our mathematical system contains a dimensionless parameter which we call the “galactic rotation number” that represents the gross ratio of centrifugal force and gravitational force. The value of this galactic rotation number is determined as part of the numerical solution. Through a systematic computational analysis, we have illustrated that the galactic rotation number remains within $\pm 10\%$ of 1.70 for a wide variety of rotation curves. This implies that the total mass in a disk galaxy is proportional to $V_0^2 R_g$, with V_0 denoting the characteristic rotation velocity (such as the “flat” value in a typical rotation curve) and R_g the radius of the galactic disk. The predicted total galactic mass of the Milky Way is in good agreement with the star-count data.

Key words: galaxy: disk — galaxies: general — galaxies: kinematics and dynamics — galaxies: structure — methods: numerical and analytical

1 INTRODUCTION

Observations have shown that a galaxy is a stellar system consisting of a massive gravitationally bound assembly of stars, an interstellar medium of gas and cosmic dust, etc. Many (mature spiral) galaxies share a common structure with the *visible* matter distributed in a flat thin disk, rotating about their center of mass in nearly circular orbits. The behavior of the stellar systems such as galaxies is believed to be determined by Newton’s laws of motion and Newton’s law of gravitation (Binney & Tremaine 1987). Thus, modeling the Newtonian dynamics of thin-disk galaxies is of fundamental importance

to our understanding of the so-called “galaxy rotation problem”—an apparent discrepancy between the observed rotation of galaxies and the predictions of Newtonian dynamics as generally perceived in the community of astrophysics (e.g., Freeman & McNamara 2006; Rubin 2006, 2007; Bennett et al. 2007).

Although scientifically well-established, the actual modeling of Newtonian dynamics, when applied to thin-disk galaxies, appeared in various forms in the literature with inconsistent conclusions. Without rigorous justification, some authors (e.g., Rubin 2006, 2007; Bennett et al. 2007; Sparke & Gallagher 2007; Keel 2007) tempted for simplicity to apply formulas based on Keplerian dynamics to the thin-disk galaxies. Theoretically, Keplerian dynamics can be derived from Newtonian dynamics as a special case for spherically symmetric gravitational systems such as the solar system and, therefore, is not expected to provide accurate descriptions for thin-disk galaxies. Hence, serious efforts were made for integrating the Poisson equation with mass sources distributed on a disk, as summarized by Binney & Tremaine (1987). The solution directly obtained from such efforts is the gravitational potential which can yield the gravitational force by taking its gradient. In an axisymmetric disk rotating at steady state, the gravitational force (the radial gradient of gravitational potential) is expected to equate to the centrifugal force due to rotation at every point.

However, solving the disk-potential problem does not seem to be a trivial pursuit. Traditional methods involved either treating the disk as a flattened spheroid that consists of a series of thin homoeoids each having a uniform density (e.g., Brandt 1960; Mestel 1963; Cuddeford 1993) or using the summation of modified Bessel functions for the potential (e.g., Toomre 1963; Freeman 1970; Nordsieck 1973; Cuddeford 1993; Conway 2000). Although seemingly elegant when derived in analytical formulas, those methods could yield closed-form solutions only for a few special cases (e.g., Mestel 1963; Freeman 1970; Binney & Tremaine 1987). But for determining the mass distribution in a galactic disk from the measured rotation curve that could have a variety of shapes, numerical integrations must be carried out and practical difficulties arise when those traditional analytical formulas are used. For example, the flattened spheroid approach via Abel integral and its inversion intrinsically restricts the “vertical” mass distribution in the disk’s axial direction to that dictated by the homoeoid structure rather than that from observations (e.g., according to van der Kruit & Searle 1982, the scale heights of galactic disks are nearly independent of radius). It is rather cumbersome to compute the surface mass density by integrating the mass density in spheroidal shells and the “spheroid” methods often lead to erroneous results for angular momentum analysis (cf. Toomre 1963; Nordsieck 1973). The Bessel function approach leads to an integral extending to infinity, whereas the observed rotation curve always ends at a finite distance. Thus, it becomes necessary to construct orbital velocity beyond the observation limit based on various assumptions (e.g., Nordsieck 1973; Bosma 1978; Jalocha, Bratek, & Kutschera 2008). Moreover, the derivative of rotation velocity usually appearing in the Bessel function formulation for computing mass density tends to introduce significant errors in practical applications.

In general, the fundamental solution to the Poisson equation (that governs the gravitation potential) is called Green’s function (Arfken 1985; Cohl & Tohline 1999). The potential from arbitrarily distributed sources can be obtained by integrating the Green’s function—serving as the integral kernel—multiplied by the source density throughout the region where the sources are located. Thus, considering the gravitational potential in terms of Green’s function is the most direct approach for realistic modeling the galactic rotation dynamics (e.g., Eckhardt & Pestaña 2002; Pierens & Huré 2004; Huré & Pierens 2005). For sources distributed axisymmetrically on a thin disk, the Green’s function can be expressed in terms of the complete elliptic integral of the first kind (e.g., Binney & Tremaine 1987). Because the dynamics of thin-disk galactic rotation is typically described along the midplane ($z = 0$) with the mass distribution being symmetric about the disk midplane and about its central axis, the radial gradient of potential in the midplane must be evaluated. The elliptic integrals of the first kind and second kind that appear in the radial gradient of potential can become mathematically singular at the midplane (when $z = 0$) where the radius of the source approaches that of the observation point. Such singularities have been considered “inconvenient from the point of view of numerical work” by Binney & Tremaine (1987) and “bothersome” by Eckhardt & Pestaña (2002). Methods were suggested to circumvent such singularities by evaluating the radial gradient of potential at a vertical distance z slightly away from $z = 0$ (cf Binney & Tremaine 1987; Eckhardt & Pestaña 2002), which seem to be somewhat *ad hoc* by nature

and lack of desirable mathematical elegance. On the other hand, it is the axisymmetric mass distribution within an idealized rotating infinitesimally thin disk that has often been of practical interest especially for rotation curve analysis (Toomre 1963). Therefore, the efforts of effectively dealing with the singularities arising from elliptic integrals has been continuously made for robust and accurate computations of the disk galaxy rotation problem (even up to recent years, e.g., Eckhardt & Pestaña 2002; Pierens & Huré 2004; Huré & Pierens 2005, 2009).

In the present work, we derive a numerical model for computing the Newtonian dynamics of thin-disk galactic rotation that allows the mass to be distributed even in an infinitesimally thin region around the midplane of the disk with the governing equation being considered strictly along the midplane ($z = 0$) and the singularities from elliptic integrals treated rigorously based on the concept of the mathematical limit. To enable dealing with arbitrary forms of rotation curves and mass density distributions, we adopt the techniques developed with boundary element method (cf. Sladek & Sladek 1998; Gray 1998; Sutradhar, Paulino & Gray 2008) for solving integral equations using compactly supported basis functions instead of that extending to infinity like Bessel functions, as detailed in Section 2. Hence the finite physical problem domain for disks of finite sizes can be conveniently considered, without the need of speculated rotation curve beyond the “cut-off” radius and evaluation of the derivative of rotation velocity. By nondimensionalizing the governing equations, a dimensionless parameter which we call the “galactic rotation number” appears in the force balance (or centrifugal-equilibrium) equation, representing the gross ratio of centrifugal force and gravitational force. We show that together with a constraint equation for mass conservation, the value of this galactic rotation number can be determined as part of the numerical solution, with computational examples presented in Section 3. With a known value of the galactic rotation number, the total galactic mass can be determined from measured galactic radius and characteristic rotation velocity, as shown in Section 4 wherefrom important physical insights are discussed.

2 MATHEMATICAL FORMULATION AND COMPUTATIONAL TECHNIQUES

For convenience of mathematical treatment, we represent a rotating galaxy by a self-gravitating continuum of axisymmetrically distributed mass in a circular disk with an edge at finite radius R_g , as shown in Fig. 1. This kind of continuum representation is typically valid when the distributed masses are viewed on a scale that is small compare to the size of the galaxy, but large compared to the mean distance between stars. Without loss of generality, we consider the thin disk having a uniform thickness (h) with a variable mass density (ρ) as a function of radial coordinate (r). Because we consider the situation of thin disk, the vertical distribution of mass (in the z -direction) is expected to contribute inconsequential dynamical effect especially as the disk thickness becomes infinitesimal. In mathematical terms, the meaningful variable here is actually the surface mass density $\sigma(r) \equiv \rho(r) h$. Whether to consider the surface mass density $\sigma(r)$ or the bulk mass density $\rho(r)$ in the mathematical equations is really a matter of taste, since they can easily be converted to each other using a constant factor h by our definition. In the present work, we use the bulk density $\rho(r)$ for its consistency with the direct physical perception of a thin disk with a nonzero thickness h .

Physically, the stars in a galaxy must rotate about the galactic center to maintain the disk-shape mass distribution. Without the centrifugal effect due to rotation, the stars would collapse into the galactic center as a result of the gravitational field among themselves. According to Binney & Tremaine (1987), it is also reasonable to assume the galaxy is in an approximately steady state with the gravitational force and centrifugal force balancing each other, in view of the fact that most disk stars have completed a large number of revolutions.

2.1 Governing Equations

Instead of following the traditional approach by first solving gravitational potential from the Poisson equation, we derive the governing equation directly from the consideration of force balance. Here, the force density on a test mass at the point of observation ($r, \theta = 0$) generated by the gravitational attraction

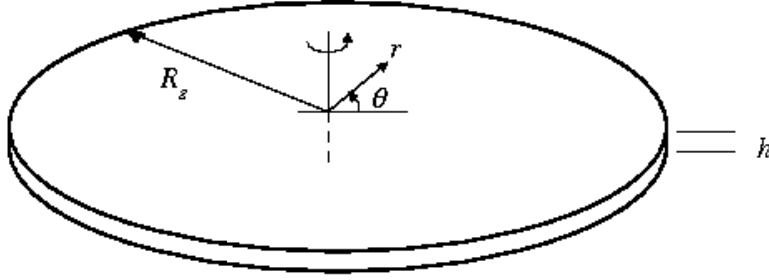


Fig. 1 Definition sketch of the thin-disk model considered in the present work. The mass is assumed to distribute axisymmetrically in the circular disk of uniform thickness h with a variable density as a function of radial coordinate r (but independent of the polar angle θ).

due to the summation (or integration) of a distributed mass density $\rho(\hat{r})$ at position described by the variables of integration $(\hat{r}, \hat{\theta})$ is expressed as an integral over the entire disk, with the distance between $(r, \theta = 0)$ and $(\hat{r}, \hat{\theta})$ given by $(\hat{r}^2 + r^2 - 2\hat{r}r \cos \hat{\theta})^{1/2}$ and the vector projection given by $(\hat{r} \cos \hat{\theta} - r)$. Thus, the equation for gravitational force to balance the centrifugal force at each and every point in a thin disk can be written as (according to Newton's laws)

$$\int_0^1 \left[\int_0^{2\pi} \frac{(\hat{r} \cos \hat{\theta} - r) d\hat{\theta}}{(\hat{r}^2 + r^2 - 2\hat{r}r \cos \hat{\theta})^{3/2}} \right] \rho(\hat{r}) h \hat{r} d\hat{r} + A \frac{V(r)^2}{r} = 0, \quad (1)$$

where all the variables are made dimensionless by measuring lengths (e.g., r, \hat{r}, h) in units of the outermost galactic radius R_g , disk mass density ρ in units of M_g/R_g^3 with M_g denoting the total galactic mass, and rotation velocities $V(r)$ in units of the a characteristic galactic rotational velocity V_0 (usually defined according to problem of interest, e.g., such as the maximum velocity corresponding to the flat part of a rotation curve). The disk thickness h is assumed to be constant and small in comparison with the galactic radius R_g . Our results for surface mass density $\rho(r) h$ are expected to be insensitive to the exact value of this ratio as long as it is small. There is no difference in terms of physical meaning between the notations (r, θ) and $(\hat{r}, \hat{\theta})$; but mathematically the former denotes the independent variables in the integral equation (1) whereas the latter the variables of integration. The gravitational force represented as the summation of a series of concentric rings is described by the first (double integral) term while the centrifugal force by the second term in (1).

Our process of nondimensionalization of the force-balance equation yields a dimensionless parameter, which we call the ‘‘galactic rotation number’’ A , as given by

$$A \equiv \frac{V_0^2 R_g}{M_g G}, \quad (2)$$

where $G (= 6.67 \times 10^{-11} \text{ (m}^3 \text{ kg}^{-1} \text{ s}^{-2}\text{)})$ denotes the gravitational constant, R_g is the outermost galactic radius, and V_0 is the characteristic velocity (which is equated here to the maximum asymptotic rotational velocity). This galactic rotation number A simply indicates the relative importance of centrifugal force versus gravitational force.

Equation (1) can either be used to determine the surface mass density $\rho(r)h$ from a given rotation curve $V(r)$ or vice versa. But when both $\rho(r)$ and A are unknown, another independent equation is needed to have a well-posed mathematical problem. According to the law of conservation of mass, the total mass of the galaxy M_g should be constant satisfying the constraint

$$2\pi \int_0^1 \rho(\hat{r})h\hat{r}d\hat{r} = 1. \quad (3)$$

This constraint can be used for determining the value of galactic rotation number A while (1) for $\rho(r)$. Equations (1)-(3) can in principle be used to determine the mass density distribution $\rho(r)$ in the disk, the galactic rotation number A , and the total galactic mass M_g , all from measured values of $V(r)$, R_g , V_0 , and h . On the other hand, if $\rho(r)$ and h (or $\rho(r)h$) are known, $V(r)$ can of course be determined from (1).

Moreover, it is known that the integral with respect to $\hat{\theta}$ in (1) can be written as

$$\int_0^{2\pi} \frac{(\hat{r} \cos \hat{\theta} - r)d\hat{\theta}}{(\hat{r}^2 + r^2 - 2\hat{r}r \cos \hat{\theta})^{3/2}} = 2 \left[\frac{E(m)}{r(\hat{r} - r)} - \frac{K(m)}{r(\hat{r} + r)} \right], \quad (4)$$

where $K(m)$ and $E(m)$ denote the complete elliptic integrals of the first kind and second kind, with

$$m \equiv \frac{4\hat{r}r}{(\hat{r} + r)^2}. \quad (5)$$

Thus, (1) can be expressed in a simpler form

$$\int_0^1 \left[\frac{E(m)}{\hat{r} - r} - \frac{K(m)}{\hat{r} + r} \right] \rho(\hat{r})h\hat{r}d\hat{r} + \frac{1}{2}AV(r)^2 = 0, \quad (6)$$

which is more suitable for the boundary element type of numerical implementation (with the double integral converted to a single integral).

2.2 Computational techniques

Following a standard boundary element approach (e.g., Sladek & Sladek 1998; Gray 1998; Sutradhar, Paulino & Gray 2008), the governing equations (6) and (3) can be discretized by dividing the one-dimensional problem domain $0 \leq r \leq 1$ into a finite number of line segments called (linear) elements. Each element covers a subdomain confined by two end nodes, e.g., element n corresponds to the subdomain $[r_n, r_{n+1}]$, where r_n and r_{n+1} are nodal values of r at nodes n and $n+1$, respectively. On each element, which is mapped onto a unit line segment $[0, 1]$ in the ξ -domain (i.e., the computational domain), ρ is expressed in terms of the linear basis functions as

$$\rho(\xi) = \rho_n(1 - \xi) + \rho_{n+1}\xi, \quad 0 \leq \xi \leq 1, \quad (7)$$

where ρ_n and ρ_{n+1} are nodal values of ρ at nodes n and $n+1$, respectively. Similarly, the radial coordinate \hat{r} on each element is also expressed in terms of the linear basis functions by so-called isoparametric mapping:

$$\hat{r}(\xi) = \hat{r}_n(1 - \xi) + \hat{r}_{n+1}\xi, \quad 0 \leq \xi \leq 1. \quad (8)$$

If the rotation curve $V(r)$ is given (from observational measurements), the N nodal values of $\rho_n = \rho(r_n)$ are determined by solving N independent residual equations over $N - 1$ element obtained from the collocation procedure, i.e.,

$$\sum_{n=1}^{N-1} \int_0^1 \left[\frac{E(m_i)}{\hat{r}(\xi) - r_i} - \frac{K(m_i)}{\hat{r}(\xi) + r_i} \right] \rho(\xi)h\hat{r}(\xi) \frac{d\hat{r}}{d\xi} d\xi + \frac{1}{2}AV(r_i)^2 = 0, \quad i = 1, 2, \dots, N, \quad (9)$$

with

$$m_i(\xi) \equiv \frac{4\hat{r}(\xi)r_i}{[\hat{r}(\xi) + r_i]^2}, \quad (10)$$

where $\rho(\xi) = \rho_n(1-\xi) + \rho_{n+1}\xi$. The value of A can be solved by the addition of the constraint equation

$$2\pi \sum_{n=1}^{N-1} \int_0^1 \rho(\xi) h \hat{r}(\xi) \frac{d\hat{r}}{d\xi} d\xi - 1 = 0. \quad (11)$$

Thus, we have $N + 1$ independent equations for determining $N + 1$ unknowns. The mathematical problem is well-posed. The set of linear equations comprising (9) and (11) for $N + 1$ unknowns (i.e., N nodal values of ρ_n and A), once computed with appropriate treatments of the mathematical singularities shown in Appendix A, can be transformed into a matrix form using the Newton-Raphson method and then solved with a standard matrix solver, e.g., by Gauss elimination in one step without further iterations (Press et al. 1988).

3 COMPUTATIONAL EXAMPLES

As we mentioned before, equations (9) and (11) can be used to either solve for $\rho(r)$ and A from a given rotation curve $V(r)$ or determine the rotation curve $V(r)$ from a given surface mass density distribution $\sigma(r) = \rho(r)h$. Usually, solving for $\rho(r)$ from a given rotation curve $V(r)$ requires computation of a linear algebra matrix problem whereas determining $V(r)$ from a given $\rho(r)$ only involves a straightforward integration. But in a spiral galaxy it is the rotation curve that can be measured with considerable accuracy; therefore, the observed rotation curve has been regarded to provide the most reliable means for determining the distribution of gravitating matter therein (Toomre 1963; Sofue & Rubin 2001). Hence, we first consider examples of solving for $\rho(r)$ and A from a given $V(r)$.

3.1 Mass distribution for rotation curve of typical shape

To obtain numerical solutions, the value of (constant) disk thickness h must be provided; we assume $h = 0.01$, which is typical of disk galaxies like the Milky Way. For computational efficiency, we distribute more nodes in the regions (e.g., near the galactic center and disk edge) where ρ has a greater gradient of variations. The typical number of nonuniformly distributed nodes N used in the computation is 1001 with which we found for most cases to be sufficient for obtaining a smooth curve of ρ versus r and discretization-insensitive values of galactic rotation number A . When numerically integrating element-by-element in (9) and (11), we use ordinary 6-point Gaussian quadrature for integrals with respect to $0 \leq \xi \leq 1$. The two-dimensional integrals (A.4) on a singular element are calculated numerically by ordinary 6×6 -point Gaussian quadrature on a unit square with $0 \leq \eta \leq 1$ and $0 \leq \xi \leq 1$.

The measurements of galactic rotation curve of mature spiral galaxies reveal that the rotation velocity $V(r)$ typically rises linearly from the galactic center in a small core and then bend down to reach an approximately constant value extending to the galactic periphery (Rubin & Ford 1970; Roberts & Whitehurst 1975; Bosma 1978; Rubin, Ford, & Thonnard 1980). These basic features may be mathematically idealized as

$$V(r) = 1 - e^{-r/R_c}, \quad (12)$$

where the dimensionless orbital velocity $V(r)$ is measured in units of the characteristic velocity V_0 defined as the maximum orbital velocity, and the parameter R_c can serve as the scale of the ‘‘core’’ of a galaxy. As shown in Fig 2, close to the galactic center when r/R_c is small, we have $V(r) \sim r/R_c$ describing a linearly rising rotation velocity (by virtue of the Taylor expansion of e^{-r/R_c}). The initial slope of this rising rotation velocity is given by $1/R_c$. Thus, larger value of R_c leads to a more gradual rise of the rotation velocity and a shrinking ‘‘flat’’ part of rotation curve which seems to disappear for $R_c \geq 0.2$.

Corresponding to the rotation curves in Fig 2 as described by (12), the computed mass density distributions in galactic disk are shown in Fig. 3. For $R_c \leq 0.02$, the curves of ρ versus r approach an

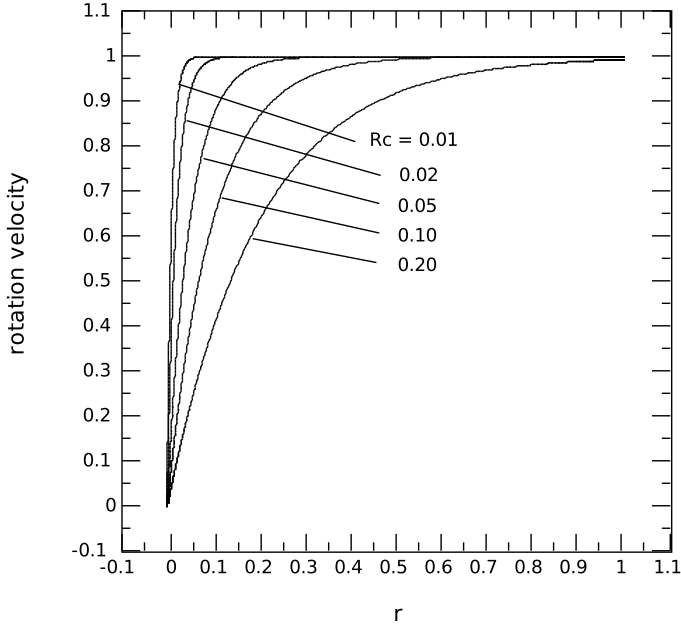


Fig. 2 Nondimensionalized orbital velocity profiles $V(r)$ according to mathematically idealized description (12) for $R_c = 0.01, 0.02, 0.05, 0.1, \text{ and } 0.2$.

asymptotic one for the most part except in a tiny region around galactic center where the peak density value at $r = 0$ still increases with further decreasing R_c . In other words, the mass density tends to decrease rapidly from the galactic center (with a slope becoming steeper for a tighter galactic core with a smaller R_c). However, beyond $r = R_c$, the mass density decrease more gradually towards the galactic periphery until reaching the galactic edge where it takes a sharp drop. Outside the galactic core ($r > R_c$), only for $R_c > 0.1$ do changes in mass density distribution and the value of A become noticeable with varying R_c . Noteworthy here is that the computed values of galactic rotation number A for $R_c \leq 0.15$ are within a small interval $[1.5708, 1.6422]$ despite orders of magnitude of R_c variation. It appears that as $R_c \rightarrow 0$ the value of A approaches a limit at ~ 1.5708 . For example, the computed results show that $A = 1.57085$ and 1.57080 for $R_c = 0.005$ and 0.001 , respectively. But the increase of A with R_c becomes more significant for $R_c > 0.15$, as illustrated by the computed results at $R_c = 0.2$ and 0.3 yielding $A = 1.7098$ and 1.9224 , respectively.

At the limit of $R_c \rightarrow 0$, the (idealized) rotation curve as described by (12) approaches a completely flat one $V(r) = 1$ (except in the infinitesimal neighborhood of $r = 0$). The solution at this limit should approach that of the well-known Mestel's disk (Mestel 1963) given by

$$\rho(r) = \frac{A}{2\pi hr} \left[1 - \frac{2}{\pi} \sin^{-1}(r) \right], \quad (13)$$

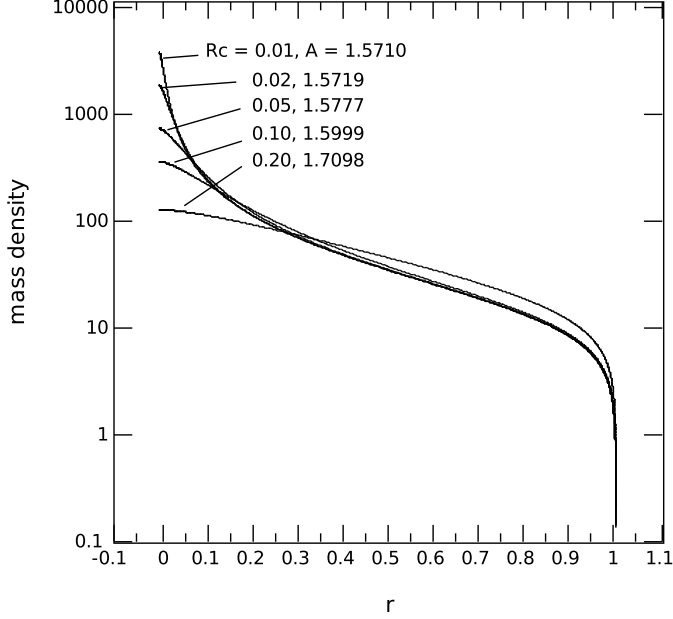


Fig. 3 The distributions of mass density $\rho(r)$ computed for $R_c = 0.01, 0.02, 0.05, 0.1,$ and 0.2 with $A = 1.5710, 1.5719, 1.5777, 1.5999,$ and 1.7098 determined as part of the numerical solutions.

in a dimensionless form consistent with the nomenclature of the present work. Here, according to (3) the galactic rotation number A can be determined by

$$A = \frac{1}{\int_0^1 \left[1 - \frac{2}{\pi} \sin^{-1}(\hat{r})\right] d\hat{r}} = \frac{\pi}{2} = 1.5707963. \quad (14)$$

As a test, we can substitute $\rho(r)$ given by (13) into (9) and (11) and compute with our code for numerical integrations to determine $V(r)$ and A . With the first node at $r = 0$ being ignored to avoid the numerical difficulties with the singularity of ρ in (13), we can indeed obtain a flat $V(r) = 1$ throughout the entire interval $(0, 1]$ (except in an infinitesimal neighborhood around $r = 0$) and $A = 1.57081$. The computed curve of ρ versus r corresponding to (13) with $A = 1.57081$ overlaps that of $R_c = 0.01$ in Fig 3 (except in the infinitesimal neighborhood of $r = 0$), as expected. This exercise demonstrates our code capability for determining the rotation curve from a given disk mass distribution, and also in a way verifies the correctness of our computational code implementation. Since most Sb galaxies—intermediate type of spiral galaxies—have rotation curves typically with a very steep rise in a small central core region, the mass density distribution in those Sb galaxies (including the Milky Way) is expected to be reasonably approximated by that of the Mestel disk (13). But for less massive Sc galaxies having more gradual rise rotation curves, their mass density distributions can deviate noticeably from that of the Mestel disk especially toward the galactic center, as shown in Fig 3 for those with $R_c > 0.02$.

3.2 Rotation curve for given mass distribution

As demonstrated in Section 3.1, numerically computing the integration in (9) for a given $\rho(\hat{r})$ as that of Mestel's disk can produce a completely flat rotation curve. Actually, rotation curves similar to those in Fig 2 can also be produced by a combination of the Freeman exponential disk and Mestel disk. Here, the Freeman disk has a surface mass density proportional to e^{-r/\tilde{R}_d} with \tilde{R}_d denoting a scale length for the exponential disk (Freeman 1970). But the Freeman exponential disk alone is known not to be able to produce a rotation curve with considerable flat portion as often being observed in disk galaxies (e.g., Freeman 1970; Binney & Tremaine 1987). The case of $V(r)$ for the Freeman exponential disk can also be computed with our code, as a check; the result showed excellent agreement with that of Freeman's analytical formula. If we use the Freeman disk for describing the galactic core having a rising rotation velocity and Mestel disk for the outer flat part, there is a good chance to obtain rotation curves of typically observed shapes. For example, we can simply construct a mass density model (which we call the Freeman-Mestel model) as

$$\rho(r) = \begin{cases} \rho_0 e^{-r/\tilde{R}_d}, & 0 \leq r < \tilde{R}_c \\ \frac{A}{2\pi h r} \left[1 - \frac{2}{\pi} \sin^{-1}(r)\right], & \tilde{R}_c \leq r \leq 1 \end{cases}, \quad (15)$$

where

$$\tilde{R}_d = \left\{ \frac{1}{\tilde{R}_c} + \frac{2}{\pi \sqrt{1 - \tilde{R}_c^2 [1 - 2 \sin^{-1}(\tilde{R}_c)/\pi]}} \right\}^{-1}$$

and

$$\rho_0 = \frac{A}{2\pi h \tilde{R}_c e^{-\tilde{R}_c/\tilde{R}_d}} \left[1 - \frac{2}{\pi} \sin^{-1}(\tilde{R}_c)\right],$$

so that both ρ and $d\rho/dr$ are continuous at the connecting point $r = \tilde{R}_c$. Moreover, the mass conservation constraint (11) can be used to determine the value of galactic rotation number as

$$A = \left[2\pi \sum_{n=1}^{N-1} \int_0^1 \rho^*(\xi) h \hat{r}(\xi) \frac{d\hat{r}}{d\xi} d\xi \right]^{-1}, \quad (16)$$

where ρ^* comes from that given by (15) by setting $A = 1$.

Although \tilde{R}_c here also serves as a scaling parameter for the galactic core, having a similar physical meaning as R_c in (12), the value of \tilde{R}_c does not have any mathematical relationship with that of R_c . For example, at $\tilde{R}_c = 0.05$ (15) and (16) yield $V(r)$ and $\rho(r)$ in Figs 4 and 5 noticeably different from those in Figs 2 and 3. For smaller values of \tilde{R}_c , the differences between $\rho(r)$ given by the Freeman-Mestel model and that in Fig 3 at the same values of R_c are less visually discernable. But the value of A determined by the Freeman-Mestel model can still be slightly different. For example, at $\tilde{R}_c = R_c = 0.01$ (16) yields $A = 1.5777$ whereas that computed in Section 3.1 is $A = 1.5710$. It seems for a given value of $\tilde{R}_c = R_c$ the rotation curve of the Freeman-Mestel model has a greater slope for the rising velocity in galactic core but a somewhat less flat velocity outside the core, as shown in Fig 4. Such a numerical difference tends to diminish with diminishing \tilde{R}_c , e.g., we have $A = 1.57147, 1.57084, \text{ and } 1.57081$ for $\tilde{R}_c = 10^{-3}, 10^{-4}, \text{ and } 10^{-5}$, respectively. As expected, $A \rightarrow 1.57080$ as that for the Mestel disk given in (14) at the limit of $\tilde{R}_c \rightarrow 0$.

What we try to illustrate here is that for obtaining rotation curves with basic observed features, a simple analytical mass density model as constructed by combination of those of Mestel (1963) and Freeman (1970) in (15) seems to be quite reasonable and convenient. In terms of computational efforts, it is usually much easier and faster to compute the rotation velocity $V(r)$ from a given mass density distribution $\rho(r)$ than vice versa. This is because that computing $V(r)$ for a known $\rho(r)$ does not need to solve the matrix problem. However, there has not been reliable means for directly measuring the

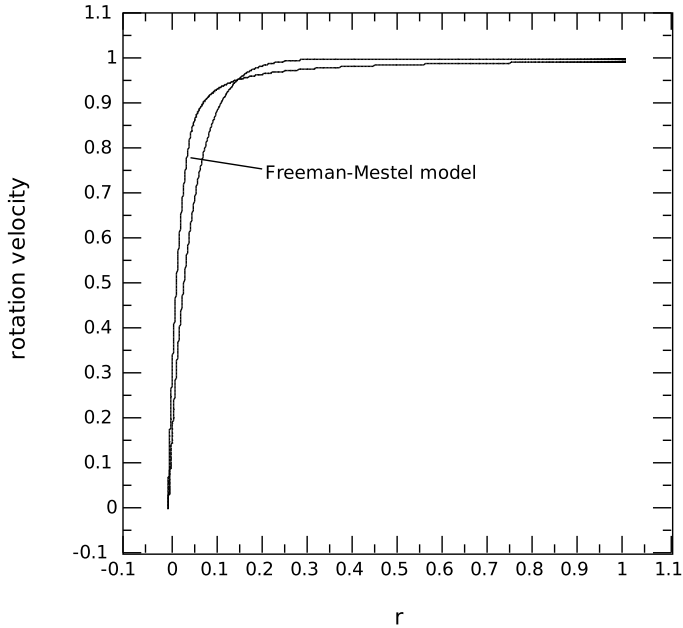


Fig. 4 The rotation velocity $V(r)$ determined with $\rho(r)$ given by (25) for the Freeman-Mestel model at $\tilde{R}_c = 0.05$, compared with that in Fig 2 for $R_c = 0.05$.

mass distribution in a disk galaxy. The mass distribution derived from measured luminosity must rely on assumed mass-to-luminosity ratio, with the validity of which being a subject of debate. Thus, accurately measured rotation curves remain as the most reliable basis for determining the distribution of mass in disk galaxies, providing fundamental information for understanding the stellar dynamics in galactic disks (Sofue & Rubin 2001).

3.3 Analysis of measured rotation curves of arbitrary shapes

For rotation curves with “idealized” shapes expressed in terms of simple mathematical functions like that in (12), we have shown that the numerically computed mass density distribution $\rho(r)$ approaches that of Mestel’s disk (13) when the galactic core is small, e.g., for $R_c \leq 0.02$. But some measured rotation curves can vary significantly from those described by simple mathematical functions or those produced by conveniently constructed mass density functions like with the Freeman-Mestel model (15).

To determine the mass density distribution according to Newtonian dynamics from a measured rotation curve of arbitrary shape, our computational scheme based on sound mathematical foundation as presented in Section 2 (as well as Appendix A) can become a generally applicable and flexible tool for many practical applications. As an example, here in Figs 6 and 7 we show our computed mass density distributions for a few actually measured galactic rotation curves with noticeably different characteristics.

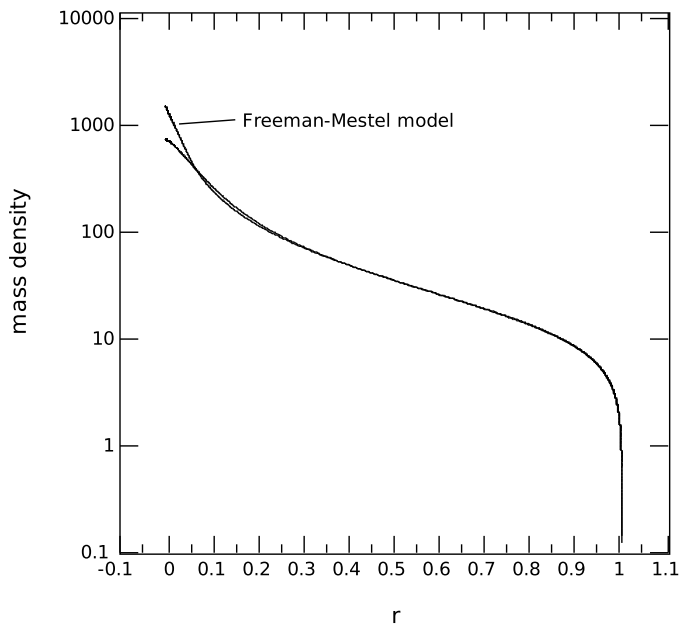


Fig. 5 The distribution of mass density $\rho(r)$ given by (25) for the Freeman-Mestel model at $R_c = 0.05$ with $A = 1.6060$, compared with that in Fig 3 for $R_c = 0.05$ with $A = 1.5777$.

The measured rotation curve for the Milky Way in Fig 6 seems to be just a few bumps and wiggles superposed on that in Fig 2 for $R_c = 0.01$. Therefore, it is no surprise to see that the corresponding mass density curve for the Milky Way in Fig 7 also exhibits a few bumps and wiggles around that in Fig 3 for $R_c = 0.01$. Similarly, the measured rotation curve for NGC 3198 in Fig 6 appears to be just that in Fig 2 for $R_c = 0.05$ with some small perturbations, and so does the computed NGC 3198 mass density in Fig 7 compared with that for $R_c = 0.05$ in Fig 3. But the rotation curve for NGC 2708 in Fig 6 differs significantly from those of typical shapes in Fig 2. The computed mass density distribution for NGC 2708 in Fig 7 shows noticeably different features from those in Fig 3. The sharp rise of mass density forward galactic center corresponds to a fast dropping of rotation velocity, as required for the force balance in Newtonian dynamics. The gradual increase in the rotation velocity in the middle section (0.1, 0.7) of NGC 2708 leads to a slow decreasing local mass density. Then a slight reduction of the rotation velocity toward the galactic periphery is responsible for a faster decrease of local mass density in the outer region $r > 0.7$ than those for flat rotation curves in Fig 7 for NGC 2708.

Despite the differences in rotation curves in Fig 6, the computed values of galactic rotation number A for these three galaxies are quite close within a few percents, namely, $A = 1.564$, 1.619 , and 1.644 , respectively for the Milky Way, NGC 3198, and NGC 2708. This is consistent with that shown in Fig 3 for a wide range of R_c . Thus, we may reasonably conclude that for most disk galaxies, the value of galactic rotation number is expected to be within $\pm 10\%$ of $A = 1.70$, with smaller A for the galaxies having high-density core and small R_c and larger A for those having more gradual rise in the rotation curve with larger R_c .

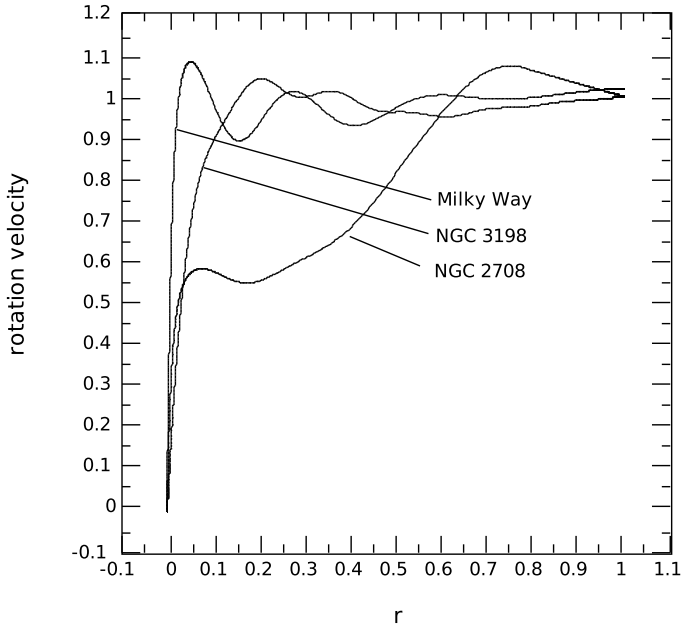


Fig. 6 The rotation curves $V(r)$ of Milky Way with $V_0 = 2.2 \times 10^5$ (m s^{-1}) and $R_g = 4.73 \times 10^{20}$ (m), NGC 3198 with $V_0 = 1.5 \times 10^5$ (m s^{-1}) and $R_g = 9.24 \times 10^{20}$ (m), and NGC 2708 with $V_0 = 2.3 \times 10^5$ (m s^{-1}) and $R_g = 1.42 \times 10^{20}$ (m).

Although we only computed examples with a few representative rotation curves, such as those described by the idealized formula (12) with several values of R_c and those actually measured with different characteristics, we believe the cases examined here actually cover a wide enough range of observational measurements that our results can offer general physical insights. Cases with rotation curves falling either close to or in between those illustrated here are not expected to differ considerably from our present findings.

4 DISCUSSION

The problem of determining the mass distribution in a thin axisymmetric disk from observed circular velocities has been investigated by many authors over the past fifty years, through various mathematical approaches. Yet satisfactory method for accurate computation is still lacking, despite the galactic rotation model has been simplified as much as possible for concisely describing only the most essential features. The main obstacle here appears to have been due to the mathematical singularities in the elliptic integrals that are apparently difficult to handle. Here in this work, we present an efficient, robust computational method with appropriate mathematical treatments such that the apparent difficulties associated with the singularities are completely removed. Thus, we are enabled to systematically analyze the basic features in a rotating disk galaxy, with properly nondimensionalized mathematical formulations. Further refinement of the present galactic rotation model may provide description of some of the fine details such as the spiral arm structure with non-axisymmetric motion (Koda & Wada 2002), gas

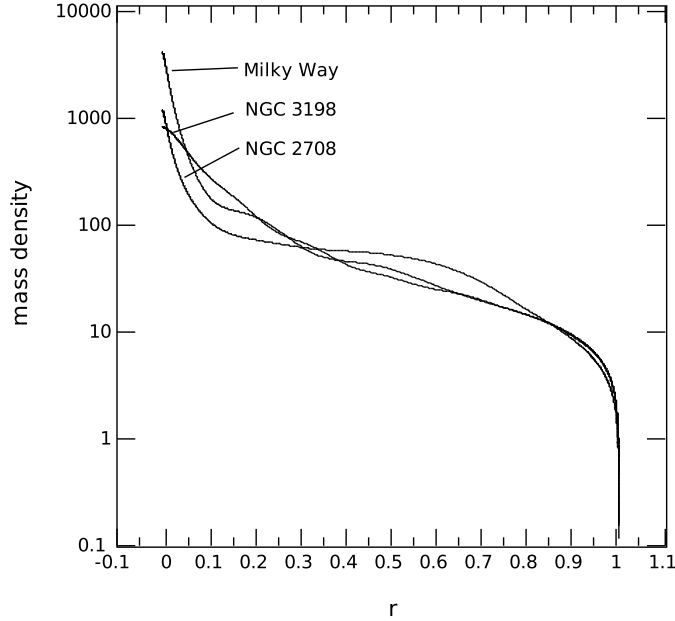


Fig. 7 The computed mass density distributions $\rho(r)$ from given rotation curves in Fig 6 for Milky Way, NGC 3198, and NGC 2708, with the values of A determined as 1.564, 1.619, and 1.644, respectively.

pressure effect in the central core (Dalcanton & Stilp 2010), disk thickness effect (Casertano 1983), etc. But those fine details should not alter the basic features significantly, at least in a gross qualitative sense. Our results in Fig 7 show that the general shape of the mass density distribution remains quite similar for rotation curves of drastically different appearances. The value of the galactic rotation number A does not change more than $\pm 10\%$ for a variety of rotation curves, indicating that the gross balance between the centrifugal force and gravitational force in a disk galaxy is usually insensitive to fine details.

4.1 Total mass in galactic disk

In the dimensionless form as presented here, our mathematical system contains a dimensionless parameter called galactic rotation number A . This galactic rotation number, with its value determined as part of the computational solution, can provide a unique insight into the dynamical system of rotating galaxy. From the knowledge of V_0 and R_g from measured rotation curves, we can determine the value of total mass M_g based on computed value of A (cf. (2)) as

$$M_g = \frac{V_0^2 R_g}{AG}. \quad (17)$$

According to the rotation curve of the Milky Way in Fig 6, we have the galactic rotation number $A = 1.564$. Then, from the measured values $V_0 = 2.2 \times 10^5$ (m s⁻¹) and $R_g = 5 \times 10^4$ (light-years)

= 4.73×10^{20} (m) (which is about 15.3 kpc where $1 \text{ kpc} = 3.086 \times 10^{19}$ m), (17) yields

$$M_g = 2.19 \times 10^{41} (\text{kg}) = 1.10 \times 10^{11} (\text{solar-mass}). \quad (18)$$

(Here, 1 solar-mass = 1.98892×10^{30} kg.) This value is in very good agreement with the Milky Way star counts of 100 billion (Sparke & Gallagher 2007).

Another example in Figs 6 and 7 is the galaxy NGC 3198, with $V_0 = 1.5 \times 10^5$ (m s^{-1}) and $R_g = 30$ (kpc) = 9.24×10^{20} (m) (Begeman 1987, 1989). Using the computed $A = 1.619$, we obtain $M_g = 1.925 \times 10^{41}$ (kg) = 9.68×10^{10} (solar-mass).

For a small disk galaxy NGC 6822, we have a rotation curve similar to that described by $R_c \sim 0.3$ in (12), with $V_0 = 6.0 \times 10^4$ (m s^{-1}) and $R_g = 5$ (kpc) = 1.54×10^{20} (m) (Weldrake et al. 2003). If we take $A = 1.92$ for $R_c = 0.3$, (17) yields $M_g = 4.33 \times 10^{39}$ (kg) = 2.18×10^9 (solar-mass).

Because the value of A does not vary much for a large range of rotation curves with various shapes (see, e.g., Figs 6 and 7), what (17) implies is that $M_g \propto V_0^2 R_g$ as what Bosma (1978) found from evaluating mass versus size in a large number of observed disk galaxies. For a fixed value of V_0 , $M_g \propto R_g$. Therefore, a disk galaxy cannot physically extend indefinitely in size, for M_g to remain finite. In other words, there must be an edge of the galactic disk at a finite radius R_g , where the mass density precipitously diminishes. Normally, one would define R_g as the radial distance where the ‘‘luminous’’, ‘‘visible’’, or ‘‘detectable’’ signal for rotating matter ends. With the advance in measurement technology using different emission lines, the detectable rotating matter (in the form of gas) seems to extend further out from the optically visible disk (cf. Sofue & Rubin 2001). Thus, the value of R_g may change with the evolving astronomical observation technology. Wherever the true R_g is located, it must correspond to an abruptly steep decrease of mass density whereas the mass density variation within R_g is expected to be smooth, according to our Newtonian dynamics model for thin-disk galaxies with typical rotation curves. It should be noted that although for a given rotation curve with fixed V_0 the total mass M_g of the galactic disk increases linearly with R_g , the dimensional value of surface mass density should generally decrease with R_g according to $1/R_g$ because it scales as M_g/R_g^2 .

As an interesting exercise, we may take (13) for the convenience in estimating the surface mass density $\sigma(r) \equiv \rho(r) h$ around the Sun in the Milky Way when R_g increases. Then, we obtain $\sigma(r_{sun}) = 0.3106, 0.7954, \text{ and } 1.7532$ for $r_{sun} = 0.5229, 0.2614, \text{ and } 0.1307$, respectively for $R_g = 15.3, 30.6, \text{ and } 61.2$ (kpc) assuming the Sun is located at $r_{sun} R_g = 8$ (kpc) from the galactic center. Based on the value given by (18), we have the dimensional surface mass density $\sigma(r_{sun}) M_g/R_g^2 \approx 146$ (solar-mass pc^{-2}) for $R_g = 15.3$ (kpc). If R_g for the flat rotation curve were found to be at 30.6 or 61.2 (kpc), the dimensional surface mass density would become 187 or 206 (solar-mass pc^{-2}), varying much less dramatically than the value of R_g . This phenomenon is a consequence of the $1/r$ part of (13), which becomes more dominant for smaller values of r . In fact, if the surface mass density $\sigma(r)$ were strictly to follow a distribution $\propto 1/r$, the dimensional surface mass density for a given dimensional radial coordinate rR_g would remain constant because the value of A changes little if at all. Thus, as R_g extends further out, the value of dimensional surface mass density in the neighborhood of Sun is expected to become almost independent of the value of R_g .

4.2 Computed mass density versus observed surface brightness

Observations of disk galaxies suggest that the surface brightness—the total stellar luminosity emitted per unit area of the disk—is approximately an exponential function of radius (Freeman 1970; Binney & Tremaine 1987). This exponential approximation seems to be especially good for the outer part of disk galaxies where the inner bulge component diminishes (e.g., Freeman 1970). Our computed mass density distributions in Fig 3 according to typical flat rotation curves indeed show nearly straight-line shape in the log-linear plots corresponding to approximately exponential function for a large portion of the problem domain, e.g., in the interval (0.2, 0.9). In fact, the least-square fit of our computed $\ln \rho$ versus r for the case of $R_c = 0.01$ (cf. Fig 3) to a linear function for $0.2 \leq r \leq 0.9$ yields

$$\ln \rho = 5.2614 - 3.4377 r, \quad (19)$$

with the correlation coefficient “ R^2 ” being 0.9968 suggesting that the portion of mass density in (0.2, 0.9) can indeed be well described by an exponential function $\rho = \rho_0 e^{-r/R_d}$ with $\rho_0 = 192.75$ and $R_d = 0.2909$. If the same least-square fitting were done for $0.1 \leq r \leq 0.9$, we would have $\rho_0 = 238.41$ and $R_d = 0.2668$ but with a slightly reduced correlation coefficient $R^2 = 0.9870$, which still indicates a good approximation with the exponential function. However, the dimensional “radial scale length” $R_d R_g$ for the Milky Way would be ~ 4.5 (or 4.1) (kpc) according to $R_d = 0.2909$ (or 0.2668) assuming $R_g = 15.3$ (kpc). This is larger than the radial scale length 2.5 (kpc) from fitting the brightness measurement data reported by Freudenreich (1998). For NGC 3198 with $R_g = 30$ (kpc), we would have $R_d R_g = 8.73$ (or 8.00) (kpc), again larger than the radial scale length of 2.63 (kpc) for the luminosity profile (cf. Begeman 1987, 1989). So, our computed results suggest that the surface mass density decreases toward the galactic periphery at a slower rate than that of the luminosity density. In other words, the mass-to-light ratio in a disk galaxy is not a constant; it generally increases with the radial distance from the galactic center as indicated by our analysis for the exponential portion of mass density distribution (which was also suggested by Bosma 1978).

But it is known that the constructed mass density distribution in terms of a single exponential function cannot generate an observed flat rotation curve (Freeman 1970; Binney & Tremaine 1987). The sharp increase of the mass density near the galactic center that drastically deviates the exponential description for $0.1 \leq r \leq 0.9$ or $0.2 \leq r \leq 0.9$ seems to play an important role for keeping the rotation curve flat forward the galactic center up to the edge of the core. In reality, most disk galaxies also have a central bulge with apparently high concentration of stars. Our pure disk model does not explicitly treat the bulge as a separate object; instead, the gravitational effect of the bulge is lumped in the rotating disk. Thus, our computed mass density should be regarded as a combination of that from the pure disk and the effective bulge represented in the disk form. This sharp increase of the disk mass density near the galactic center can be considered as an account for the highly concentrated mass in the central bulge. Actually, it may not be impossible to extend the formulation in Section 3.2 for a mass density distribution to include a summation (or expansion) of several exponential terms with different radial scales lengths, for matching an observed rotation curve with more complicated shape. Yet, the most straightforward method for determining the mass density distribution for a given rotation curve (of arbitrary shape) is by numerically solving the linear algebra matrix equation derived based on sound mathematical ground for disk galaxies of finite size as presented in Section 2 and demonstrated in Section 3.1 and Section 3.3.

4.3 Inaccuracy of Keplerian dynamics for disk galaxies

Enchanted by its simplicity, the Keplerian dynamics was applied by several authors in description of the disk galaxy behavior without seriously inquiring its validity and accuracy. To clarify some of the problems in such an over-simplification, here we present a quantitative analysis of the fundamental differences between the Keplerian dynamics and Newtonian dynamics especially when applied to disk galaxies.

From analyzing the orbits of planets around the Sun, Kepler empirically discovered laws for planet motion in the solar system. It was Newton who mathematically showed that Kepler’s laws are actually consequences of Newton’s laws of motion and universal law of gravitation. The so-called Keplerian dynamics can be derived from Newton’s theorems for the gravitational potential of any spherically symmetric mass distribution. In considering the balance between gravitational force from the distributed mass in a galaxy and centrifugal force due to rotation, applying Keplerian dynamics would lead to an equation as

$$\frac{2\pi}{r^2} \int_0^r \rho(\hat{r}) h \hat{r} d\hat{r} - A \frac{V(r)^2}{r} = 0, \quad (20)$$

which is apparently quite different from (1) as rigorously derived for the thin-disk galaxies. However, the force balance equation based on Keplerian dynamics (20) looks much simpler than that of Newtonian dynamics (1). If justifiable in a quantitative sense, it may be conveniently used as a reasonable approxi-

mation to the more involved rigorous computations. To provide a quantitative comparison, we herewith examine a few basic mathematical features of (20) to illustrate whether the Keplerian dynamics can be practically used as a reasonable approximation to the Newtonian dynamics (1) for disk galaxies.

For a given rotation curve with the orbital velocity $V(r)$ described by (12), an analytical solution to (20) for $\rho(r)$ can be obtained as

$$\rho(r) = \frac{A}{2\pi h} \left[\frac{1}{r} \left(1 - 2e^{-r/R_c} + e^{-2r/R_c} \right) + \frac{2}{R_c} \left(e^{-r/R_c} - e^{-2r/R_c} \right) \right]. \quad (21)$$

Thus, (21) describes a mass density approaching $3Ar/(2\pi h R_c^2) \rightarrow 0$ as $r \rightarrow 0$ with a positive slope for small r yet approaching $A/(2\pi h r)$ as $r \rightarrow 1$ (because e^{-1/R_c} can be negligibly small for small R_c , e.g., $e^{-1/R_c} = 4.54^{-5}$, 2.06×10^{-9} , and 1.93×10^{-22} for $R_c = 0.1, 0.05$, and 0.02 , respectively). The mass density distribution of (21) does not monotonically decrease with r as that shown in Fig 3; instead, it is zero at the galactic center and increases for small r according to a slope $\propto 1/R_c^2$ (which can be large for small R_c) until reaching a peak value, then decreases in a form $\propto 1/r$ towards the galactic periphery $r = 1$ without the precipitous drop seen in Fig 3.

Substituting (21) to (3) yields

$$A = \frac{1}{1 - 2e^{-r/R_c} + e^{-2r/R_c}}, \quad (22)$$

which leads to $A \approx 1$ for small R_c , quite different from 1.57 when $R_c \rightarrow 0$ as obtained in Section 3.1. Hence using the Keplerian dynamics to describe the disk galaxies can be misleading, because not only the results differ quantitatively but also qualitatively from that based on rigorous computations.

On the other hand, if we assume the mass density distribution is known, e.g., as that given by (13), (20) leads to

$$V(r)^2 = \frac{1}{r} \int_0^r \left[1 - \frac{2}{\pi} \sin^{-1}(\hat{r}) \right] d\hat{r} = 1 - \frac{2}{\pi} \left[\sin^{-1}(r) - \frac{1 - \sqrt{1 - r^2}}{r} \right].$$

Instead of a completely flat rotation curve, the Mestel's disk mass density distribution with Keplerian dynamics would yield orbital velocity $V(r)$ that monotonically decreases with r , having $V(0) = 1$ and $V(1) = 0.7979$. Therefore, a mass density distribution corresponding to a flat rotation curve based on Newtonian dynamics would be mistaken as failing to explain the observed flat rotation curve when Keplerian dynamics were inappropriately employed, because it instead predicts a falling rotation curve.

5 CONCLUSIONS

In the present paper, we show that with appropriate mathematical treatments the apparent difficulties associated with singularities in computing elliptic integrals can be eliminated when modeling Newtonian dynamics of thin-disk galactic rotation. Using the well-established boundary element techniques, the nondimensionalized governing equations for disks of finite sizes can be discretized, transformed into a linear algebra matrix equation, and solved by straightforward Gauss elimination in one step without further iterations. Although the mathematical derivations in Appendix A for removing the singularities seem somewhat sophisticated, the actual implementations of the numerical code are not as lengthy. With our code on a typical personal computer with a single Pentium 4 processor, each solution in Section 3 takes no more than a minute or so to compute. Thus, a numerical code implemented according to our algorithm can be conveniently used to accurately determine the surface mass density distribution in a disk galaxy from a measured rotation curve (or vice versa), which is important for in-depth understanding of the Newtonian dynamics and its capability of explaining the ‘‘galaxy rotation problem’’ via rotation curve analysis. Moreover, the dimensionless galactic rotation number A in our mathematical system can provide important insights into the general dynamical behavior of disk galaxies.

Through a systematic computational analysis, we have illustrated that the value of the galactic rotation number remains within $\pm 10\%$ of $A = 1.70$ for a wide variety of rotation curves. For most Sb type

galaxies like the Milky Way, having rotation curves typically with a very steep rise in a small central core region and a large range of flat portion, we have showed that $A \approx 1.60$ with a surface mass density very close to that of Mestel's disk (except in an infinitesimal neighborhood of the galactic center where the Mestel disk becomes singular). But for galaxies with "non-ideal" rotation curves containing considerable irregularities, our numerical approach can easily be used without modification for computing the corresponding surface mass density distributions accurately for rotation curve analysis.

Because the value of $A \equiv V_0^2 R_g / (M_g G)$ remains almost invariant for various galaxies, we can draw a conclusion that the total mass in a disk galaxy M_g must be proportional to $V_0^2 R_g$. For galaxies with similar characteristic rotation velocity V_0 , their total mass M_g must be proportional to their disk size R_g . Our model predicts that at the disk edge the surface mass density is expected to diminish precipitously whereas within the disk edge the surface mass density should vary rather smoothly without sharp changes except near the galactic center. Thus, a disk galaxy with a finite amount of mass must also have a finite size, based on the Newtonian dynamics modeling.

For a disk galaxy with a typical flat rotation curve, our modeling result show that the surface mass density monotonically decreases from the galactic center toward periphery, according to Newtonian dynamics. In a large portion of the galaxy, the surface mass density follows an approximately exponential law of decay with respect to the galactic radial coordinate. Yet the radial scale length for the exponential portion of surface mass density seems to be generally larger than that of the measured exponential brightness distribution, suggesting an increasing mass-to-light ratio with the radial distance in a disk galaxy. This is consistent with typical edge-on views of disk galaxies often revealing a dark edge against a bright background bulge.

ACKNOWLEDGEMENTS

We are indebted to Dr. Len Gray of Oak Ridge National Laboratory for teaching detailed boundary element techniques for elegant removal of various singularities in integral equations. We want to thank Dr. Louis Marmet for his intuitive discussion and preliminary computational results that convinced us to pursue a rigorous numerical analysis of the galactic rotation problem. The results shared by Ken Nicholson, Prof. Michel Mizony for computing the similar problem should also be acknowledged for enhancing our confidence.

Appendix A: TREATMENTS OF SINGULAR ELEMENTS

The complete elliptic integrals of the first kind and second kind can be numerically computed with the formulas (Abramowitz & Stegun 1972)

$$K(m) = \sum_{l=0}^4 a_l m_1^l - \log(m_1) \sum_{l=0}^4 b_l m_1^l \quad (\text{A.1})$$

and

$$E(m) = 1 + \sum_{l=1}^4 c_l m_1^l - \log(m_1) \sum_{l=1}^4 d_l m_1^l, \quad (\text{A.2})$$

where

$$m_1 \equiv 1 - m = \left(\frac{\hat{r} - r}{\hat{r} + r} \right)^2. \quad (\text{A.3})$$

Clearly, the terms associated with $K(m_i)$ and $E(m_i)$ in (9) become singular when $\hat{r} \rightarrow r_i$ on the elements with r_i as one of their end points.

The logarithmic singularity can be treated by converting the singular one-dimensional integrals into non-singular two-dimensional integrals by virtue of the identities:

$$\begin{cases} \int_0^1 f(\xi) \log \xi d\xi = - \int_0^1 \int_0^1 f(\xi\eta) d\eta d\xi \\ \int_0^1 f(\xi) \log(1 - \xi) d\xi = - \int_0^1 \int_0^1 f(1 - \xi\eta) d\eta d\xi \end{cases}, \quad (\text{A.4})$$

where $f(\xi)$ denotes a well-behaving (non-singular) function of ξ on $0 \leq \xi \leq 1$.

But a more serious non-integrable singularity $1/(\hat{r} - r_i)$ exists due to the term $E(m_i)/(\hat{r} - r_i)$ in (9) as $\hat{r} \rightarrow r_i$. The $1/(\hat{r} - r_i)$ type of singularity is treated by taking the Cauchy principle value to obtain meaningful evaluation (cf. Kanwal 1996), as commonly done with the boundary element method (Sladek & Sladek 1998; Gray 1998; Sutradhar, Paulino & Gray 2008). In view of the fact that each r_i is considered to be shared by two adjacent elements covering the intervals $[r_{i-1}, r_i]$ and $[r_i, r_{i+1}]$, the Cauchy principle value of the integral over these two elements is given by

$$\lim_{\epsilon \rightarrow 0} \left[\int_{r_{i-1}}^{r_i - \epsilon} \frac{\rho(\hat{r}) \hat{r} d\hat{r}}{\hat{r} - r_i} + \int_{r_i + \epsilon}^{r_{i+1}} \frac{\rho(\hat{r}) \hat{r} d\hat{r}}{\hat{r} - r_i} \right]. \quad (\text{A.5})$$

In terms of elemental ξ , (A.5) is equivalent to

$$- \lim_{\epsilon \rightarrow 0} \left\{ \int_0^{1 - \epsilon/(r_i - r_{i-1})} \frac{[\rho_{i-1}(1 - \xi) + \rho_i \xi][r_{i-1}(1 - \xi) + r_i \xi] d\xi}{1 - \xi} - \int_{\epsilon/(r_{i+1} - r_i)}^1 \frac{[\rho_i(1 - \xi) + \rho_{i+1} \xi][r_i(1 - \xi) + r_{i+1} \xi] d\xi}{\xi} \right\}. \quad (\text{A.6})$$

Performing integration by parts on (A.6) yields

$$\rho_i r_i \log \left(\frac{r_{i+1} - r_i}{r_i - r_{i-1}} \right) - \left(\int_0^1 \frac{d\{[\rho_{i-1}(1 - \xi) + \rho_i \xi][r_{i-1}(1 - \xi) + r_i \xi]\}}{d\xi} \log(1 - \xi) d\xi + \int_0^1 \frac{d\{[\rho_i(1 - \xi) + \rho_{i+1} \xi][r_i(1 - \xi) + r_{i+1} \xi]\}}{d\xi} \log \xi d\xi \right),$$

where the two terms associated with $\log \epsilon$ cancel out each other, the terms with $\epsilon \log \epsilon$ become zero at the limit of $\epsilon \rightarrow 0$, and the first term becomes nonzero when the mesh nodes are not uniformly distributed (namely, the adjacent elements are not of the same segment size). In other words, inclusion of this first term enables the usage of nonuniformly distributed nodes for more effective computations, which is one of the algorithm improvements over that in our previous works (Gallo & Feng 2009, 2010).

At the galaxy center $r_i = 0$ (i.e., $i = 1$),

$$\int_{r_i}^{r_{i+1}} \frac{\rho(\hat{r}) \hat{r} d\hat{r}}{\hat{r} - r_i} = \int_0^{r_{i+1}} \rho(\hat{r}) d\hat{r}. \quad (\text{A.7})$$

Thus, the $1/(\hat{r} - r_i)$ type of singularity disappears naturally. However, numerical difficulty can still arise if ρ itself becomes singular as $r \rightarrow 0$, e.g., $\rho \propto 1/r$ as for the Mestel disk (Mestel 1963). The singular mass density at $r = 0$ corresponds to a mathematical cusp, which usually indicates the need of finer resolution in the physical space. To avoid the cusp in mass density at the galactic center, we can impose a requirement of continuity of the derivative of ρ at the galaxy center $r = 0$. This be easily implemented at the first node $i = 1$ to demand $d\rho/dr = 0$ at $r = 0$. In discretized form for $r_1 = 0$ we simply have

$$\rho(r_1) = \rho(r_2). \quad (\text{A.8})$$

When $r_i = 1$ (i.e., $i = N$), we are at the end node of the problem domain. Here we use a numerically relaxing boundary condition by considering an additional element beyond the domain boundary covering the interval $[r_i, r_{i+1}]$, because it is needed to obtain a meaningful Cauchy principle value. In doing so we can also assume $r_{i+1} - r_i = r_i - r_{i-1}$ such that $\log[(r_{i+1} - r_i)/(r_i - r_{i-1})]$ becomes zero, to simplify the numerical implementation. Moreover, it is reasonable to assume $\rho_{i+1} = 0$ because it is located outside the disk edge where the extremely low intergalactic mass density is expected to have inconsequential gravitational effect. With sufficiently fine local discretization, this extra element

can be considered to cover a diminishing physical space such that its existence becomes numerically inconsequential. Thus, at $r_i = 1$ (where $i = N$) we have

$$\int_0^1 \frac{d\{\rho_i(1-\xi) + \rho_{i+1}\xi\}[r_i(1-\xi) + r_{i+1}\xi]}{d\xi} \log \xi d\xi$$

$$= (\rho_{i+1} - \rho_i) \int_0^1 r(\xi) \log \xi d\xi + (r_{i+1} - r_i) \int_0^1 \rho(\xi) \log \xi d\xi = \rho_i[r_i - \frac{3}{2}(r_i - r_{i-1})].$$

Now that only logarithmic singularities are left, (A.4) can be used to eliminate all singularities in computing the integrals in (9).

Noteworthy here is that the (removable) singularities in the kernels of the integral equation (6), when properly treated, lead to a diagonally dominant Jacobian matrix with bounded condition number in the Newton-Raphson formulation (Press et al. 1988). This fact makes the matrix equation robust for any straightforward matrix solver.

References

- Abramowitz, M. & Stegun, I. A. 1972, Handbook of Mathematical Functions. Dover, New York
- Arfken, G. 1985, Mathematical Methods for Physicists, 3rd edn. Academic Press, Orlando
- Begeman, K. G. 1987, PhD thesis, Groningen University; 1989, A&A, 223, 47
- Bennett, J., Donahue, M., Schneider, N. & Voit, M. 2007, Cosmic Perspective: Stars, Galaxies, and Cosmology. Addison and Wesley, San Francisco
- Binney, J. & Tremaine, S. 1987, Galactic Dynamics. Princeton University Press, Princeton
- Bosma, A. 1978, The Distribution and Kinematics of Neutral Hydrogen in Spiral Galaxies of Various Morphological Types, PhD Thesis, Rijksuniversiteit Groningen
- Brandt, J. C. 1960, ApJ, 131, 293
- Casertano, S. 1983, MNRAS, 203, 735
- Cohl, H. S. & Tohline, J. E. 1999, ApJ, 527, 86
- Conway, J. T. 2000, MNRAS, 316, 540
- Cuddeford, P. 1993, MNRAS, 262, 1076
- Dalcanton, J. J. & Stilp, A. M. 2010, ApJ, 721, 547
- Eckhardt, D. H. & Pestaña, J. L. G. 2002, ApJL, 572, L135
- Faber, S. M. & Gallagher, J. S. 1979, A&A, 17, 135
- Freeman, K. C. 1970, ApJ, 160, 811
- Freeman, K. C. & McNamara, G. 2006, In Search of Dark Matter. Springer, Berlin
- Freudenreich, H. T. 1998, ApJ, 492, 495
- Gallo, C. F. & Feng, J. Q. 2009, in Potter, F., eds, 2nd Crisis in Cosmology Conference (APS Conference Series Vol 413) p. 288
- Gallo, C. F. & Feng, J. Q. 2010, J. Cosmology, 6, 1373
- Gray, L. J. 1998, in Sladek, V. and Sladek, J., eds, Singular Integrals in Boundary Element Method (Advances in Boundary Elements Series Vol 3). Computational Mechanics Publishers, p. 33
- Huré, J.-M. & Pierens, A. 2005, ApJ, 624, 289
- Huré, J.-M. & Pierens, A. 2009, A&A, 507, 573
- Jalocha, J.-M., Bratek, L. & Kutschera, M. 2008, ApJ, 679, 373
- Kanwal, R. P. 1996, Linear Integral Equations: Theory and Technique. Birkhauser, Boston
- Keel, W. C. 2007, The Road to Galaxy Formation, 2nd edn. Springer
- Koda, J. & Wada, K. 2002, A&A, 396, 867
- Mestel, L. 1963, MNRAS, 126, 553
- Nordsieck, K. H. 1973, ApJ, 184, 719
- Pierens, A. & Huré, J.-M. 2004, ApJ, 605, 179
- Press, W. H., Teukolsky, S. A., Vetterling, W. T. & Flannery, B. P. 1988, Numerical Recipes. Cambridge University Press, Cambridge

- Roberts, M. S. & Whitehurst, R. N. 1975, *ApJ*, 201, 327
- Rubin, V. C. 2006, *Phys. Today*, 59 (12), 8
- Rubin, V. C. 2007, *Phys. Today*, 60 (9), 8
- Rubin, V. C. & Ford, Jr., W. K. 1970, *ApJ*, 159, 379
- Rubin, V. C., Ford Jr., W. K. & Thonnard, N. 1980, *ApJ*, 238, 471
- Sladek, V. & Sladek, J. 1998, in Sladek, V. and Sladek, J., eds, *Singular Integrals in Boundary Element Method (Advances in Boundary Elements Series Vol 3)*. Computational Mechanics Publishers, p. 1
- Sofue, Y. & Rubin, V. C. 2001, *Ann. Rev. Astron. Astrophys.*, 39, 137.
- Sparke, L. S. & Gallagher, III., J. S. 2007, *Galaxies in the Universe*, 2nd edn. Cambridge University Press, Cambridge
- Sutradhar, A., Paulino, G. H. & Gray, L. J. 2008, *Symmetric Galerkin Boundary Element Method*. Springer, Berlin
- Toomre, A. 1963, *ApJ*, 138, 385
- van der Kruit, P. C. & Searle, L. 1982, *A&A*, 110, 61
- Weldrake, D. T. F., de Blok, W. J. F. & Walter, F. 2003, *MNRAS*, 340, 12